HHS Public Access

Author manuscript

ACS Appl Mater Interfaces. Author manuscript; available in PMC 2021 April 01.

Published in final edited form as:

ACS Appl Mater Interfaces. 2020 March 25; 12(12): 13644–13656. doi:10.1021/acsami.9b22474.

Controlled Delivery of Curcumin and Vitamin K2 from Hydroxyapatite-Coated Titanium Implant for Enhanced in Vitro Chemoprevention, Osteogenesis, and in Vivo Osseointegration

Naboneeta Sarkar,

W. M. Keck Biomedical Materials Research Laboratory School of Mechanical and Materials Engineering, Washington State University, Pullman, Washington 99164, United States

Susmita Bose

W. M. Keck Biomedical Materials Research Laboratory School of Mechanical and Materials Engineering, Washington State University, Pullman, Washington 99164, United States

Abstract

Successful repair of critical-sized tumor-resection defects, especially in load-bearing bones, still remains a major challenge in clinical orthopedics. Titanium (Ti) implants have been increasingly used in the past few decades because of titanium's suitable mechanical properties and biocompatibility; however, it shows insufficient integration with the surrounding bone. In this study, the plasma spray technique is utilized to form homogeneous hydroxyapatite (HA) coating on the surface of the Ti implant to enhance osseointegration at the tissue-implant interface. These coated implants are loaded with curcumin and vitamin K2 to introduce chemopreventive and osteogenesis ability via controlled release of these biomolecules. The synergistic effect of these two biomolecules showed enhanced in vitro osteoblast (hFOB) cell attachment and proliferation for 11 days. Moreover, these biomolecules showed lower in vitro osteosarcoma (MG-63) cell proliferation after 3, 7, and 11 days. An in vivo study was carried out to evaluate the bone bonded zone in a rat distal femur model at an early wound healing stage of 5 days. Modified Masson Goldner staining of the tissue-implant section showed improved contact between tissue and implant in dual drug-loaded HA-coated Ti implants compared to control implants. This work presents a successful fabrication of a mechanically competent functional Ti implant with the advantages of enhanced in vitro osteoblast proliferation, osteosarcoma inhibition, and in vivo osseointegration, indicating the potential for load-bearing bone-defect repair after tumor resection.

Graphical Abstract

Corresponding Author: **Susmita Bose** – Phone: (509) 335-7461; sbose@wsu.edu.

Complete contact information is available at: https://pubs.acs.org/10.1021/acsami.9b22474

The authors declare no competing financial interest.

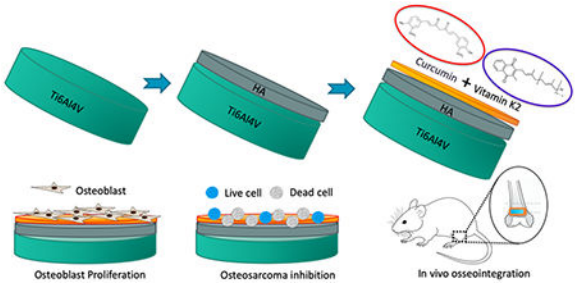

Keywords

curcumin; vitamin K2; plasma-coated Ti6Al4V; osteoblast; osteosarcoma; in vivo

1. INTRODUCTION

Osteosarcoma is the most common primary bone malignancy with the third highest incidence rate in pediatric patients.[1] It is an aggressive form of tumor, which advances with rapid growth and infiltration and, subsequently, metastasizes to other body parts, predominantly to the lungs.[2] Currently, the standard treatment regimen includes a combination of pre- and postoperative chemotherapy and a surgical resection. Once a patient is diagnosed with osteosarcoma, high dosages of standard chemotherapeutic drugs, such as doxorubicin, adriamycin, or methotrexate, are administered and continued for 6–10 weeks before surgery to decrease the size of tumor.[3] Limb salvaging surgery is currently the mainstay and considered the safest methodology of treatment for 85–90% of patients with high-grade osteosarcoma, in which diseased tissue and tracts are eliminated with at least a 2 cm margin to prevent further recurrences.[4,5] After the surgery, chemotherapy is again resumed within 2–3 weeks once the wound is healed. Despite the advancements made with the current therapeutic approaches for osteosarcoma treatment, the survival rate has not altered over the past three and a half decades, even with the use of combination chemotherapy. While high dosages of chemotherapeutic agents during pre- and postoperative chemotherapy causes severe side effects and fatal toxicity because of their lack of specificity toward tumor cells,[6] surgical resection of a tumor determines large bone defects, challenging the quality of the patient's life.[7] Hence, advanced bone graft substitutes with dual functions of osteogenesis and specific chemopreventive ability are stringently needed for osteosarcoma management, which might hold the key to an improved survival rate.

Implants with a localized drug delivery system can eliminate the need for multiple surgical interventions or extensive dosing schedule by enhancing the efficacy of the eluted drug. However, current drug delivery systems are limited to the release of a single biomolecule over a continuous period of time, which does not address the situations where a complex delivery profile is required.[8] For instance, there is an unmet need for an advanced drug delivery regimen, which would provide effective chemoprevention to remove the residual bone cancer cells, as well as simultaneously endow the scaffold with unique osteogenic capability to regenerate new bone tissue. Additionally, single-drug chemotherapies are not

effective to suppress all cancer cells because of the multidrug resistance of the tumors.[9] Therefore, combination chemotherapy with multidrug delivery properties has been developed to achieve ideal therapeutic effects and improved antitumor efficacy.[10] Yet, achieving effective chemoprevention without possessing toxicity to normal cells is a great challenge in current tumor management.[11] Hence, the present study focuses on designing localized natural drug delivery system from coated implants that release multiple nontoxic biomolecules to achieve postoperative chemoprevention as well as bone defect reconstruction. This local drug delivery system adjunct to the traditional chemotherapy can minimize the systemic side effects, diminish the risk of metastasis and therefore lead to better clinical efficiency.

Curcumin, the active constituent of turmeric and a natural polyphenol compound, has instigated considerable interest for its extensive physiological activities.[12] It deserves a special mention for its success rate in the field of cancer therapeutics because of its remarkable anti-inflammatory and anticarcinogenic properties. Curcumin regulates multiple cell-signaling pathways and demonstrates significant cytotoxic potential toward a variety of tumor cells, as reported in various in vitro, in vivo, and preclinical studies.[13,14] Previous studies from our group have also reported the chemopreventive and osteogenic potential of curcumin for osteosarcoma prevention.[15] On the other hand, vitamin K2, a fat-soluble vitamin, is known for its role in diabetes, osteoporosis, osteoarthritis, and cancer prevention. It acts as an anabolic agent and, therefore, improves bone quality by stimulating bone formation and reducing bone resorption.[16,17] Besides, researches are currently pursued to identify the association of vitamin K2 and its potential effect on cancer.[18,19] These natural biomolecules-based drug deliveries are safe yet effective and mitigate systemic toxicity caused by high dosages of conventional chemotherapeutic agents.

Titanium (Ti) and its alloys have demonstrated promising potential in reconstituting bone in load-bearing sites because of their excellent biocompatibility, high mechanical strength, fracture toughness, and corrosion resistance.[20–22] However, the strong oxidized layer on the surface of titanium alloys, which provides the corrosion resistance property to the underlying substrate, also create biological inertness and hinders direct interaction of the implant with bone tissue.[23] Such problems with osseointegration at the bone/implant surface are made only more complex for patients suffering from osteosarcoma.[24] To address this issue, much effort has been focused on coating Ti implant with bioactive materials as it not only promotes bone tissue regeneration but also shortens the healing time significantly.[25–27] Among all bioceramics-based coatings, hydroxyapatite (HA) is predominantly employed as an osteogenic coating material for orthopedic implants.[28,29] It mimics the mineral phase of human cortical bone by maintaining the Ca/P ratio at 1.67, which ultimately enhances the bone-bonding ability of the Ti implant.[30] Even though poor mechanical properties and inherent brittleness of HA limits its practical application for load-bearing application, as a bioactive coating on load-bearing Ti implant, HA provides excellent osseointegration at the implant surface and, therefore, offers complementary properties to each other.[31] In this study, Ti6Al4V, which is a classical α–β dual phase titanium alloy, is utilized followed by plasma spray coating of HA. So far, plasma spraying is the only commercialized FDA (Food and Drug Administration) approved biomedical coating techniques and therefore considered the gold standard for commercial production of coated metallic implants.[32,33]

The objective of this study is to investigate the localized dual-drug delivery of curcumin and vitamin K2 from plasma-sprayed HA-coated Ti6Al4V on in vitro chemoprevention, osteogenesis, and in vivo osseointegration ability for postsurgical bone defect repair applications, especially for orthopedic devices used in load-bearing conditions. We hypothesize this simple yet efficient design of load-bearing HA-coated Ti implant offers an efficient dual drug delivery of chemopreventive and osteogenic molecule for postsurgical defect repair in osteosarcoma management.

2. MATERIALS AND METHODS

2.1. Preparation of Coating and Surface Topography Characterization.

Ti6Al4V plates (Grade 5), purchased from Titanium Joe (MA, USA), were cut by a water jet cutter into discs with a diameter of 12.2 mm and thickness of about 2 mm. Subsequently, these discs were sandblasted, cleaned ultrasonically in deionized (DI) water and treated with acetone to ensure the remaining organic material was removed. HA powder (Monsanto, MO, USA) was sieved to receive 150–212 μm particle size prior to coating. Afterward, coatings were applied using a 30 kW inductively coupled radio frequency (RF) plasma spray system (Tekna Plasma Systems, Canada). The system is equipped with a supersonic plasma nozzle and an axial powder feeding system. Twenty-five kW plate power and 110 mm working distance were maintained for this work. Argon (Ar) gas was used as the central and carrier gas with a flow rate of 25 and 13 standard liters per minute (slpm). A mixture of 60 slpm argon and 6 slpm hydrogen were used for sheath gas. Chamber pressure was kept at 5 pound-force per square inch gauge (psig). The surface topography of the samples was measured by means of a Zygo optical profilometer (Zygo Corporation, CT, USA). The surface parameter used for the evaluation of surface roughness was the arithmetic average roughness (R_a). For each replicate, 15 1 mm × 1 mm scan measurements were averaged as the final value of roughness from five separate locations of each sample.

2.2. Drug Coating.

Dual drug solution was prepared by simultaneously dissolving curcumin (≥98.0% Sigma-Aldrich, USA) and vitamin K2 (Analytical grade, Sigma-Aldrich, USA) (curcumin/vitamin K2 = 1:1) in ethanol. Curcumin was (0.5 g) dissolved in 10 mL of ethanol and stirred for 10 min, followed by the addition of 0.5 g of vitamin K2 and mixing for another 10 min. The resultant dual drug solution (500 μL) containing both curcumin and vitamin K2 was added on the top surface of the HA-coated Ti implants so that the total drug amount reached 50 μg in each disc (25 μg of curcumin and 25 μg of vitamin K2). Finally, the solvents were evaporated at room temperature by keeping the samples in the dark overnight.

2.3. In Vitro Curcumin and Vitamin K2 Release.

Curcumin and vitamin K2 release study was investigated in both pH 7.4 phosphate buffer and pH 5.0 acetate buffer. The 7.4 pH is used to imitate physiological pH, whereas 5.0 pH resembles the postsurgery acidic microenvironment. The pH range is kept within ±0.05 using a pH probe. Samples in triplicate were placed in 4 mL of buffer solution. Then they are kept at a shaker at 37 °C under 150 rpm of constant shaking. The buffer solutions were changed at each time point and replaced with freshly prepared 4 mL of buffer solution. The

concentration of curcumin was determined using Biotek Synergy 2 SLFPTAD microplate reader (Biotek, Winooski, VT, USA). The absorbance values were obtained at 425 and 248 nm wavelength for curcumin and vitamin K2, respectively, and drug concentration was calculated using a standard curve. The release kinetics were analyzed using Korsmeyer-Peppas model.[34]

$$M_t/M_\infty = K \cdot t^n$$

where M_t is the quantity of drug released at time t, M_∞ is the maximum quantity released, K is the release rate constant, and n is the release exponent, which allows to identify the drug release mechanism.

$$\ln(M_t/M_\infty) = \ln(K) + n \cdot \ln(t)$$

A graph was plotted using $\ln(M_t/M_\infty)$ versus $\ln(t)$, where n is the slope of the graph. In this study, n value of ≤0.45 is applied, which defines Fickian diffusion for cylindrical shaped matrices.

2.4. Dissolution and Surface Morphology after Release.

Field emission scanning electron microscope (FESEM) (FEI, Inc., Hillsboro, OR, USA) was used to characterize surface morphologies of all implants to observe phase dissolution after release. Before performing FESEM, the implants are left to dry at room temperature for 72 h. Then, they were gold coated using a sputter-coater (Technics Hummer V, CA, USA).

2.5. In Vitro Osteoblast and Osteosarcoma Cell Culture Study.

2.5.1. Osteoblast Cell Culture.—Prior to cell culture, all samples were sterilized by autoclaving at 121 °C for 60 min. Human osteoblast cell line hFOB (PromoCell GmbH, Germany) were used for this culture. Samples were kept in 24 well plates, and cells were seeded onto the samples at a density of 2×10^6 cells/mL. Osteoblast growth medium (PromoCell GmbH, Germany) was used to maintain the culture for the entire study. Cultures were kept in an incubator at 37 °C under an atmosphere of 5% CO_2 as recommended by PromoCell for this particular cell line. Growth medium was changed every 2 days during the entire cell culture study.

2.5.2. Osteosarcoma Cell Culture.—Prior to the in vitro cell culture study, all implants were sterilized using an autoclave (Tuttnauer, USA) at 121 °C for 60 min. Human osteosarcoma cell line (MG-63) and Eagles Minimum Essential Medium (EMEM) were purchased from ATCC, USA. Cell culture media or EMEM was replaced every 2–3 days during the entire study. Subsequently, sterilized implants were loaded with the drugs and placed in 24-well plates. Confluent cells were seeded on the implant surface at a density of 2.5×10^4 cells/sample. The implants were moved to a new well after an adhesion period of 12 h. The culture was kept in an incubator at 37 °C under an atmosphere of 5% CO_2 as recommended by ATCC for this particular cell line.

2.5.3. Cell Morphology.—To characterize cellular morphology by FESEM, samples were separated from culture after 3, 7, and 11 days of study. The samples were fixed with 2% paraformaldehyde/2% glutaraldehyde in 0.1 M cacodylate buffer overnight at 4 °C. 2% osmium tetroxide (OsO_4) is used for postfixation for 2 h at room temperature. Then, the samples were dehydrated in a series of ethanol (30%, 50%, 70%, 95%, and 100% three times), followed by hexamethyldisilane (HMDS) drying. Samples are kept in a vacuum desiccator for overnight drying. Gold coating with a thickness of 10–15 nm was applied using a gold sputter coater. The morphology of samples is then studied using FESEM (FEI 200F, FEI Inc., OR, USA).

2.5.4. MTT Cell Viability Assay.—hFOB and MG-63 cell viability was evaluated using MTT (3-(4,5-dimethylthiazol-2-yl)-2,5-diphenyl tetrazolium bromide) (Sigma, St. Louis, MO) assay. To prepare the MTT solution, 5 mg of MTT is dissolved in 1 mL of sterile-filtered PBS. 100 μL of MTT solution was then added to each sample in 24-well plates followed by the addition of 900 μL of cell medium. The samples were incubated for 2 h. One milliliter of MTT solubilizer is prepared using 10% Triton X-100, 0.1 N HCl, and isopropanol. After incubation, 600 μL of MTT solubilizer was added to dissolve the formazan crystals. Thereafter, 100 μL of that solution was transferred into a 96-well plate and read by UV–vis spectroscopy microplate reader (BioTek) at 570 nm. To ensure reproducibility, all samples were used in triplicate. Data are presented as mean ± standard deviation. Student's *t* test was used to perform statistical analyses and *P* values <0.05 and <0.0001 are considered significant and extremely significant.

2.6. In Vivo Study.

2.6.1. Surgery and Implantation Procedure.—Sprague–Dawley rats (Charles Rivers Laboratories International, Inc., Wilmington, MA, USA) with 280–320 g of body weight were used in this study. A protocol approved by the Institutional Animal Care and Use Committee (IACUC), Washington State University, was obeyed while performing the surgeries. The rats were kept in a temperature and humidity-controlled rooms with alternate cycles of 12 h dark and 12 h light. After the animals get acclimated, surgery was performed to generate a femoral defect. Anesthesia was carried out by using IsoFlo (isoflurane, USP, Abbott Laboratories, North Chicago, IL, USA), along with oxygen (Oxygen USP, A-L Compressed Gases Inc., Spokane, WA, USA). Pedal reflex and respiration rate of the rats were monitored to maintain proper surgical anesthesia. The 3/5 mm defect was created in the distal femur bone by making a through and through hole using a drill bit of 2/3 mm diameter. Physiological saline was used to cleanse the cavity and remove the remaining bone fragments present in the defect site. Thereafter, drug-loaded HA-coated Ti implant were press fitted at the defect site. Pure HA-coated Ti implants were used as control. To close the wound an absorbable synthetic surgical suture, undyed braided-coated monocryl polyglactin 910 (Ethicon Inc., Somerville, NJ, USA), was used. A betadine solution, as a disinfectant, was applied at the wound site to prevent postsurgical infection. Meloxicam injection was applied to reduce the pain after the surgery. Rats were euthanized by CO_2 overdose after 6 weeks postsurgery. The bone-implant specimens were cut from the rat body using a rotating saw and then fixed with 10% neutral buffered formalin solution for 72 h.

2.6.2. Histomorphology and Histomorphometric Analysis by Modified Masson Goldner's Trichrome (Undecalcified Tissue Sections).—

A series of dehydration process is carried out for the bone tissue specimens using ethanol (70%, 95%, and 100%), ethanol/acetone (1:1), and 100% acetone. Each step is carried out for 8–12 h. Now, the specimen is kept in acetone: Spurr's resin (2:1 and then 1:1) for infiltration. Next, the sample tube/vial is filled with acetone: Spurr's resin (1:1) and kept overnight with the lid open so the acetone evaporates. Then, 100% spurs resin is used to keep the tissue specimens. Lastly, the bone-implant specimen is kept in a mold filled with 100% Spurr's resin at 60 °C overnight. After the samples are embedded in Spurr's resin, a thin section of 200 μm is cut with the help of slow-speed diamond saw cutter and attached on a glass slide using super glue. After the slide was dried, the tissue sections were stained by Masson Goldner's trichrome stain and observed under an optical microscope (Olympus BH-2, Olympus America Inc., USA).

The histomorphometric analysis is carried out using ImageJ software (NIH) to measure percentage fraction of newly formed bone area (area covered by newly formed bone/area of the entire tissue section, %) and percentage of total bone formation. 1/1 mm tissue sections were used to measure the newly formed bone area ($n = 6$). The region around the implant assessed was 250 μm in radius using 3 different images. All analysis was normalized over the radius of the implant. Statistical significance was determined at a 95% confidence level ($p < 0.05$) marked with * between compositions and time points.

2.7. Statistical Analyses.

All in vitro experiments data are representative of three biological replicates ($n = 3$). Each of this biological replicate had three technical replicates as well. The data were normally distributed by the Shapiro–Wilk test and were represented as mean ± SD. Statistical analyses were performed in GraphPad Prism 8 software (CA, USA) using two-way ANOVA and Bonferroni posthoc analysis. P values ≥0.05 were considered as statistically significant.

3. RESULTS

3.1. Fabrication of Implant, Drug Loading, and Surface Topography Characterization.

Surface topography of the implant, or more importantly, average surface roughness is an important parameter for tissue-material responses, which significantly improves cellular attachment and proliferation. Figure 1 demonstrates schematic diagram of step by step fabrication of drug-loaded HA-coated Ti implant and surface topography of each step by optical profilometer. The result indicates that the surface roughness has increased drastically upon plasma deposition of HA as compared to Ti. HA-coated substrates with a rough surface morphology is reported to promote better hFOB attachment than smooth Ti surface. The curcumin- and vitamin K2-loaded HA-coated Ti has comparable R_a value to that of pure HA-coated Ti implants. The surface roughness and spatial parameters are shown in Table 1. For instance, the average surface roughness (R_a) value was 2.35, 10.43, and 8.61 μm for the Ti, HA-coated Ti, and drug-loaded HA-coated Ti surfaces, respectively.

3.2. In Vitro Drug Release Study at Physiological and Acidic Microenvironment.

Since pathological condition, such as cancer, exhibits different pH conditions than normal physiological pH, the drug release in our study has been conducted in tumor-specific release media. HA coating is greatly affected by the pH of the surrounding media. In general, an acidic pH results in higher solubility of HA, which subsequently instigates accelerated drug release in acidic condition. However, in our study, both the drugs, curcumin and vitamin K2, showed an overall higher release in DMEM (pH 7.4), compared to acidic buffer media (pH 5.0). Serum-containing media, such as DMEM supplemented with fetal bovine serum (FBS), is a more suitable choice for performing release studies since it mimics the critical composition of physiological fluids that are used for in vitro studies or in vivo assays. The serum proteins present in FBS affects the drug release by achieving the sink condition. As shown in Figure 2, after 22 days, 100% release of curcumin is achieved in the presence of vitamin K2 in the system, while only curcumin shows 88% of release at pH 7.4. Similarly, vitamin K2 showed enhanced drug release of 68% in the presence of curcumin in the system, while only vitamin K2 loaded samples showed 11% of drug release.

Morphological characterization of sample surface after 22 days of drug release shows a gradual degradation of the coated surface in the presence of DMEM, as shown in Figure 3. Cracks and porous morphology are observed in all samples indicating extensive degradation characteristics.

Similarly, Figure 4 shows that after 22 days of release, curcumin has shown much higher release in the presence of vitamin K2 (about 93%) compared to 30% release of drug from samples loaded with only curcumin at pH 5.0. After 22 days, vitamin K2 also showed 61% of release in the presence of curcumin, where 15% release can be seen from the samples that had only vitamin K2.

Much lower coating degradation and nonporous surface morphology is observed in the presence of acetate buffer, which is shown in Figure 5. Therefore, drug release from coated implant at acidic pH follows diffusion mechanism rather than degradation kinetics, followed by dissolution of HA. Therefore, it can be concluded that HA-coated Ti implant provides a suitable drug delivery platform, which exhibits an independent release pattern for curcumin and vitamin K2 under physiological, as well as acidic microenvironment exhibited by tumor cells.

The in vitro release kinetics were analyzed by Korsmeyer–Peppas equation to understand the release mechanism for curcumin, vitamin K2, and dual drug-loaded HA-coated Ti implants. Table 2 summarizes the Korsmeyer–Peppas model parameters, where n denotes the diffusion exponent and R^2 is the coefficient of determination, obtained from the linear regression analysis. In this study, n value of the Korsmeyer–Peppas plot was less than 0.45 for <60% of cumulative drug release kinetics. This result further validates the release mechanism for drug-loaded HA-coated Ti implants was primarily controlled by Fickian diffusion process.

3.3. In Vitro Cytotoxicity Study against Human Osteosarcoma Cells (MG-63).

To evaluate the in vitro chemopreventive effect of dual drug (curcumin + vitamin K2) release from HA-coated Ti implant, osteosarcoma cell culture was carried out at days 3, 7,

and 11. HA-coated Ti implant without any treatment was used as the control. MG-63 osteosarcoma cell attachment, proliferation, and viability were tested in the presence of control, curcumin-, vitamin K2-, and curcumin + vitamin K2-loaded HA-coated Ti implant. As shown in Figure 6a, all the treatment implants demonstrated lower osteosarcoma cell viability compared to the control, at days 3, 7, and 11. Although cell inhibition capacity of vitamin K2 was weaker than curcumin, the synergistic effect of curcumin and vitamin K2 still showed effective in vitro osteosarcoma suppression at days 7 and 11. The individual release of curcumin (0.23 $\mu g/mm^2$) exhibited 92% and 85% lower osteosarcoma cell proliferation compared to the control at days 7 and 11, respectively. However, the dual release of curcumin (0.11 $\mu g/mm^2$) and vitamin K2 (0.11 $\mu g/mm^2$) showed 95% and 92% lesser osteosarcoma cell viability at days 7 and 11, respectively. This superior chemopreventive effect can be attributed to the higher release of curcumin and vitamin K2, while present in a combination form, as shown in Figure 2. The FESEM images in Figure 6b show layer-like osteosarcoma cells in control samples, whereas curcumin and vitamin K2 both showed significant inhibition in attachment and proliferation of MG-63 cells, which is consistent with the MTT results. The in vitro percentage cytotoxicity results at days 3, 7, and 11 demonstrated effective inhibitory efficacy against human osteosarcoma cells in the presence of curcumin and vitamin K2 released from HA-coated Ti implants, as presented in Table 3.

3.4. In Vitro Osteoblast (hFOB) Cell–Material Interaction.

To verify the nontoxic effect of curcumin and vitamin K2 on healthy bone cells, osteoblast (hFOB) cell culture was carried out for 11 days. As shown in MTT assay in Figure 7a, individual release of curcumin did not show any statistically significant increment in cellular viability at days 3 and 7, compared to the control ($p > 0.05$). Nevertheless, vitamin K2-loaded HA-coated Ti implant was found to be more effective in enhancing osteoblast cellular viability than curcumin-loaded sample. In fact, it increased osteoblast cell viability to almost 3.5-fold on day 3 and 2.5-fold at day 7 in comparison to the control HA-coated Ti implant. At day 11, the effect was more pronounced with vitamin K2 (0.23 g/mm^2), showing a marked 9 folds increase in osteoblast cell viability suggesting its significant in vitro osteogenic potential. Dual release of curcumin and vitamin K2 did not show any cytotoxicity against osteoblast cell proliferation, in fact slightly increased the viability to 1.3-, 1.7-, and 1.6-fold at days 3, 7, and 11, respectively. Excellent biocompatibility of the HA-coated implants can be further confirmed by the FESEM images, as shown in Figure 7b. HA-coated Ti implants because of their inherent cytocompatibility promoted osteoblast cell adhesion and proliferation within 3 days of incubation. Although curcumin did not show notable cellular growth and layer-like proliferation, presence of few osteoblast attachment on the implant surface does confirm its noncytotoxicity toward healthy hFOB cell line. On the other hand, vitamin K2-loaded implant displayed discrete cellular morphology with filopodial processes anchored firmly on top of the scaffold surface, which indicates its superior osteogenic potential, compared to the control. Moreover, dual delivery of curcumin and vitamin K2 also demonstrated densely arranged osteoblast cells with monolayer formation and good attachment suggesting their excellent cytocompatibility and osteogenic capability.

3.5. In Vivo Surgeries and Osseointegration.

To further investigate the osteogenic potential of curcumin- and vitamin K2-incorporated HA-coated Ti implants, a 3/5 mm bicortical epicondyle defect was created in the distal femur of Sprague–Dawley rats, followed by surgical implantation and sacrifice after 5 days, shown in Figure 8a and b. The tissue sections were prepared and stained with Masson Goldner to characterize the bone bonded zone. The anteroposterior radiograph in Figure 8c is taken immediately after the femoral epicondyle implantation, which confirms no obvious abnormalities in any rats. Figure 8d shows histological characterization by Masson Goldner staining at the tissue–implant interface. Curcumin and vitamin K2 both showed evidence of significantly greater bone formation around the implant, compared to the control. These results have shown a distinctly visible effect of curcumin and vitamin K2 on osseointegration at the bone-bonded surface during early time point of wound healing, which was never reported in previous literature, as per authors best knowledge.

In vivo osseointegration ability of curcumin, vitamin K2, and curcumin + vitamin K2 were assessed by histomorphological characterization of tissue–implant sections utilizing Masson Goldner staining, as shown in Figure 9a. The results show a significantly larger gap of 380 ± 38 μm between the implant and newly forming bone tissue for control groups (HA-coated Ti implant) with no treatment. The tissue–implant contact was significantly better in curcumin and vitamin K2 incorporated HA-coated Ti implant groups. Furthermore, dual delivery of curcumin and vitamin K2 showed prominent improvement in osseointegration with the lowest gap of 50 ± 4 μm between the tissue and implant. Additionally, the presence of newly formed osteoid tissue in orange/reddish-orange color and mineralized bone formation in greenish color is more prevalent in curcumin + vitamin K2-incorporated HA-coated Ti groups, compared to the control. Histomorphometrical analysis by imageJ in Figure 9b shows almost three-fold higher osteoid and total bone formation by curcumin- and vitamin K2-loaded HA-coated Ti compared to control.

4. DISCUSSION

With the increasing incidences of bone metastasis, localized drug delivery approaches for cancer therapeutics have demonstrated a steep rise over the past few years. Although HA coatings on orthopedic implants have received much attention as load-bearing bone replacements, repair of tumor-associated segmental bone-defects remains a major challenge to orthopedic surgeons. This is due to the poor bone–implant osseointegration and difficulty in new bone formation in the tumor environment. Additionally, incomplete surgical resection results in tumor recurrence and approximately half of the patients with bone cancer eventually exhibit bone metastasis. Hence, there is a considerable interest in developing local drug delivery systems from coated implants, which could facilitate the controlled release of anticancer and osteogenic biomolecules at the tumor site for enhanced chemoprevention and faster bone regeneation.[35]

Bioactive HA coatings have been used as a drug carrier for controlled therapeutic delivery of chemopreventive agents in osteosarcoma treatment. To achieve successful drug delivery in cancer microenvironment and overall implant success, the drug release needs to be tested at pH 7.4, which simulates the in vitro testing condition and normal physiological

microenvironment, as well as at pH 5.0, which imitates the postsurgical acidic condition and extracellular microenvironment of tumor cells. In this study, the in vitro release kinetics of curcumin and vitamin K2 indicated that both drugs showed controlled and sustained drug delivery from HA-coated Ti implant at pH 7.4 and pH 5.0 for 22 days. It is worth noting that both curcumin and vitamin K2 demonstrated a primary burst release with 17% of total drug in the first 24 h. This initial burst release of drug at pH 5.0 can provide immediate eradication of residual tumor cells followed by a sustained release at physiological pH 7.4 will promote gradual healing and bone regeneration.[36] To better simulate the in vivo environment, Dulbecco's Modified Eagle medium (DMEM) solution have been used in this study to represent pH 7.4 for in vitro drug release kinetics evaluation. DMEM supplemented with FBS contains components from blood serum, organic constituents, such as vitamins, amino acids, and proteins, which helps to better simulate the in vivo environment or physiological conditions of a living body, compared to the SBF (simulated body fluid) or PBS (phosphate buffer solution) containing only inorganic components. Now, these proteins and amino acids are readily absorbed on the implant surface and results in reduced crystallinity and subsequent degradation.[37] Higher surface degradation significantly enhances the drug release from HA coating, which might be an explanation for observing an overall higher release of all drugs in pH 7.4, compared to the pH 5.0 or acetate buffer solution. In addition, a comparatively higher release was observed from both the drugs at pH 5.0 and pH 7.4 when they were combined together. It can be noted that the release of vitamin K2 was almost 6- and 4-fold higher in pH 7.4 and pH 5.0, respectively, when the combination of both drugs was incorporated. Curcumin and vitamin K2 are both aromatic fat-soluble molecules with similar chemical structure; therefore, their higher release in combined form may be attributed to the hydrophobic interaction between drug molecules, where the drug molecules aggregate together resulting in a faster diffusion from the implant surface. This enhanced release kinetics might allow curcumin and vitamin K2 to be an ideal choice for synergistic drug combination in cancer prevention.[37] Furthermore, the cumulative release kinetics for both curcumin and vitamin K2 are best fitted with the Korsmeyer–Peppas model, to further analyze the drug release kinetics. The diffusion exponent or n value from the Korsmeyer-Peppas plot for are less than 0.45 for both curcumin and vitamin K2 loaded Ti implants, which corresponds to Fickian diffusion mechanism.[38] Although this model has been previously used to define drug release profiles from polymeric matrix, nowadays various studies have reported its application in porous ceramics drug delivery system. Dissolution of HA coating is an important parameter that not only regulates the durability and stability of the coating but also controls the drug release kinetics. Previous studies have reported that the acidic condition of release media results in undesirable accelerated resorption of HA coating. Here, HA coating still maintains its physical form and integrity even after 22 days of drug release at pH 5.0, which confirms the feasibility of utilizing this drug delivery system in the tumor microenvironment.[39]

After monitoring a controlled release pattern of curcumin and vitamin K2 for 22 days, the in vitro antitumor efficacy of the drug-loaded implants was assessed. On account of the high chemopreventive potential of curcumin, the curcumin- and vitamin K2-loaded HA-coated implant exhibited excellent performance for in vitro osteosarcoma proliferation inhibition. Vitamin K2 is an emerging chemotherapeutic agent with cytotoxic potential toward a wide

variety of cancer cell lines including leukemia, pancreatic cancer, hepatocellular carcinoma, colorectal cancer, breast cancer, and ovarian cancer.[40,41] Although several in vitro, in vivo, and clinical trials have reported a promising chemotherapeutic potential of vitamin K2, investigations of the underlying mechanism of anticancer function are still in its infancy. On the other hand, curcumin has been extensively researched and well-documented for its anticancer potential. It modulates multiple cell-signaling pathways including NF-$\kappa\beta$ (nuclear factor-$\kappa\beta$ to restrict cell proliferation and tumor progression.[42] Both curcumin and vitamin K2 are regarded as potential inhibitor of NF-$\kappa\beta$, a transcription factor that plays major role in cancer cell progression and tumor growth. In resting cell, NF-$\kappa\beta$ is present in cytoplasm conjugated with I$\kappa\beta$ which keeps it in inactivated state. Phosphorylation of IKβ results in subsequent degradation, which marks the activation of NF-$\kappa\beta$ upon releasing from the conjugate. Next, activated NF-$\kappa\beta$ translocates to the nucleus, binds to DNA, and stimulates cellular proliferation. Curcumin and vitamin K2 inhibit phosphorylation and subsequent activation of NF-$\kappa\beta$, which leads to suppression of tumor cells and tumor regression.[43]

Treating tumor cells while sparing healthy cells is a critical challenge in current targeted drug delivery systems. Therefore, these implants were tested against human osteoblast cell line to ensure their noncytotoxicity toward normal bone cells. Results showed curcumin- and vitamin K2-treated HA-coated implants do not exhibit any toxicity toward osteoblast cell line and promote firm cellular attachment and proliferation. One of the key advantages of employing naturally occurring phytochemicals, such as curcumin, is their noncytotoxicity toward normal cells, which indicates fewer side effects and increased targeting efficacy of tumor cells. Curcumin has proven to exhibit no adverse effects on the human body even with high dosages of 2–12 g/day.[44] More intriguingly, curcumin has demonstrated a significant role in promoting osteoblastic differentiation of rMSCs and alleviating RANKL-induced osteoclast resorption, which accounts for its excellent performance in improving bone health.[45] Additionally, some studies also reported selective toxicity of curcumin toward osteosarcoma compared to normal osteoblast cells, a concept which is implemented in the present work to overcome the limitations of osteosarcoma management.[46] Compared to other therapeutic approaches, such as integrating bone scaffolds with a potent anticancer drug, curcumin- and vitamin K2-loaded HA-coated Ti implants represent a safer and promising alternative for treating osteosarcoma-related bone defect by providing a higher local drug concentration and mitigating adverse side effects or cytotoxicity to normal cells. Vitamin K2, an essential vitamin for bone remodeling, offers great prospects in the prevention and treatment of osteoporosis and overall maintenance of bone health.[47] Vitamin K2 is a cofactor of γ-carboxylase enzyme, which transforms inactivated glutamic acid residues (Glu) to activated γ-glutamic acid residues (Gla). Three Gla residues are present in osteocalcin (OC), which is a bone protein synthesized and secreted by osteoblast. This γ-carboxylated osteocalcin (cOC) comprises of calcium binding site that attracts calcium ion followed by incorporating them into bone forming HA crystals.[48] In addition to promoting osteoblast proliferation, maturation, and differentiation, vitamin K2 also inhibits osteoclast formation by decreasing RANKL expression and results in apoptosis of osteoclast.[49] These promising reports, accompanied by the very limited toxicity of vitamin K2 can be attributed to the excellent in vitro osteogenic performance exhibited in this study.

Considering the great osteogenic potential of the implants in vitro, further investigation was carried out to evaluate the in vivo osseointegration ability of curcumin + vitamin K2-loaded HA-coated Ti implants. To this end, femoral epicondyle defect models were created in male Sprague–Dawley rats, followed by localized implantation of HA-coated Ti implants into bone defects. The results indicate a better contact between the implant and surrounding bone tissue after 5 days of implantation, confirming high osseointegration ability of curcumin + vitamin K2-loaded HA-coated Ti implants. Although there have been plenty of reports focusing on the formation of osseous tissues on the synthetic bone graft substitutes, in vivo therapeutic outcome of such early phase of implantation is largely unknown. This desirable therapeutic outcome was attributed to the synergistic effects of curcumin and vitamin K2, which indicates a significant material guided bone regeneration process that involves adhesion and proliferation of osteoblast leading to subsequent initiation of osteoconduction and osteoinduction. In regard to this, past few years have witnessed the rapid development of curcumin as a natural biomolecule with excellent osteogenic potential accompanied by the exceptional ability to improve implant osseointegration.[50] A recent study showed improved bone volume and bone-implant contact in the presence of curcumin in a critical calvarial defect of diabetic rat.[51] More research focusing on the effect of curcumin in bone tissue engineering has revealed that surface loaded curcumin successfully reduced fibrous encapsulation in titanium implants without affecting osseointegration.[52] Curcumin also helped to reduce titanium particle-induced inflammation and thereby demonstrated its efficacy for the treatment of osteolysis and aseptic loosening.[53] Similarly, few studies have reported the beneficial effect of vitamin K2 on in vivo bone formation and subsequent improvement in bone healing around the implants.[54] In one study, combination therapy of vitamin K2 and parathyroid hormone promotes bone healing in HA-coated Ti implant by improving osseointegration, binding strength and new bone formation around the implant.[55] These results from our study confirm that curcumin and vitamin K2 sequentially serve as both chemopreventive agent and osteogenic component, which may overcome the critical challenges faced by current osteosarcoma management. In addition, they provide a therapeutic platform by integrating natural chemopreventive and osteogenic biomolecules into HA-coated Ti implant to prepare a multifunctional load-bearing implant for osteosarcoma-related bone defect repair.

5. SUMMARY

This study demonstrates the feasibility of designing load-bearing plasma-sprayed HA-coated Ti6Al4V implant with the advantages of localized delivery of biologically active molecules for enhanced chemopreventive and osteogenic properties. The HA coating enables sustained release of curcumin and vitamin K2 in both physiological pH and acidic microenvironment, as shown by in vitro release kinetics. The implants showed severe cytotoxicity against osteosarcoma cells suggesting their significant in vitro chemopreventive potential. While, the control group showed layer-like osteosarcoma cell attachment on the implant surface, the dual release of curcumin and vitamin K2 showed little to no cell attachment with 95% and 92% lower osteosarcoma cell viability compared to control, at days 7 and 11, respectively. The response of bone cells was also assessed by osteoblast cell culture, which indicates that the drug-loaded implants possess no toxicity toward hFOB, and in fact, vitamin K2

promoted osteoblast viability and proliferation to almost 9-fold at day 11. The result also highlights the enhanced in vivo osseointegration ability of curcumin- and vitamin K2-incorporated HA-coated Ti6Al4V implant after 5 days of femoral epicondyle defect surgery in rat distal femur model. Although future research is necessary to evaluate long-term osseointegration effect in large animal models, this work represents a simple yet effective development of load-bearing bone implant for applications in the repair of bone defects.

ACKNOWLEDGMENTS

Authors would like to acknowledge financial support from the National Institutes of Health under Grant R01 AR066361. The authors would like to thank Dr. Valerie Lynch-Holm from Franceschi Microscopy and Imaging Center, WSU and Dr. Arda Gozen from School of Mechanical and Materials Engineering, WSU for their help with the FESEM and optical profilometry. Authors also appreciate help with the sample preparation from Dr. Dongxu Ke, Ashley Vu and Sam Robertson.

REFERENCES

(1). Kansara M; Teng MW; Smyth MJ; Thomas DM Translational biology of osteosarcoma. Nat. Rev. Cancer 2014, 14 (11), 722. [PubMed: 25319867]

(2). Verron E; Schmid-Antomarchi H; Pascal-Mousselard H; Schmid-Alliana A; Scimeca J-C; Bouler J-M Therapeutic strategies for treating osteolytic bone metastases. Drug Discovery Today 2014, 19 (9), 1419–1426. [PubMed: 24742971]

(3). Luetke A; Meyers PA; Lewis I; Juergens H Osteosarcoma treatment–where do we stand? A state of the art review. Cancer Treat. Rev 2014, 40 (4), 523–532. [PubMed: 24345772]

(4). Palama IE; Arcadio V; D'Amone S; Biasiucci M; Gigli G; Cortese B Therapeutic PCL scaffold for reparation of resected osteosarcoma defect. Sci. Rep 2017, 7 (1), 12672. [PubMed: 28978922]

(5). Misaghi A; Goldin A; Awad M; Kulidjian AA Osteosarcoma: a comprehensive review. SICOT-J 2018, 4, 12. [PubMed: 29629690]

(6). Zhang Y; Yang J; Zhao N; Wang C; Kamar S; Zhou Y; He H; et al. Progress in the chemotherapeutic treatment of osteosarcoma. Oncology Letters 2018, 16 (5), 6228–6237. [PubMed: 30405759]

(7). Durfee RA; Mohammed M; Luu HH Review of osteosarcoma and current management. Rheumatology and therapy 2016, 3 (2), 221–243. [PubMed: 27761754]

(8). Zhang Y; Yang C; Wang W; Liu J; Liu Q; Huang F; Chu L; Gao H; Li C; Kong D; Liu Q; Liu J Co-delivery of doxorubicin and curcumin by pH-sensitive prodrug nanoparticle for combination therapy of cancer. Sci. Rep 2016, 6, 21225. [PubMed: 26876480]

(9). Li C.-j.; Liu X.-z.; Zhang L; Chen L.-b.; Shi X; Wu S.-j.; Zhao J.-n. Advances in Bone-targeted Drug Delivery Systems for Neoadjuvant Chemotherapy for Osteosarcoma. Orthopaedic surgery 2016, 8 (2), 105–110. [PubMed: 27384718]

(10). Ma H; Jiang C; Zhai D; Luo Y; Chen Y; Lv F; Yi Z; Deng Y; Wang J; Chang J; Wu C A bifunctional biomaterial with photothermal effect for tumor therapy and bone regeneration. Adv. Funct. Mater 2016, 26 (8), 1197–1208.

(11). Zhou Z-F; Sun T-W; Chen F; Zuo D-Q; Wang H-S; Hua Y-Q; Cai Z-D; Tan J Calcium phosphate-phosphorylated adenosine hybrid microspheres for anti-osteosarcoma drug delivery and osteogenic differentiation. Biomaterials 2017, 121, 1–14. [PubMed: 28063979]

(12). Hewlings S; Kalman D Curcumin: a review of its' effects on human health. Foods 2017, 6 (10), 92.

(13). Wang K; Zhang C; Bao J; Jia X; Liang Y; Wang X; Chen M; Su H; Li P; Wan J-B; He C Synergistic chemopreventive effects of curcumin and berberine on human breast cancer cells through induction of apoptosis and autophagic cell death. Sci. Rep 2016, 6, 26064. [PubMed: 27263652]

(14). Bose S; Sarkar N; Banerjee D Effects of PCL, PEG and PLGA polymers on curcumin release from calcium phosphate matrix for in vitro and in vivo bone regeneration. Materials today chemistry 2018, 8, 110–120. [PubMed: 30480167]

(15). Sarkar N; Bose S Liposome-Encapsulated Curcumin-Loaded 3D Printed Scaffold for Bone Tissue Engineering. ACS Appl. Mater. Interfaces 2019, 11 (19), 17184–17192. [PubMed: 30924639]

(16). Akbari S; Rasouli-Ghahroudi AA Vitamin K and bone metabolism: A review of the latest evidence in preclinical studies. BioMed Res. Int 2018, 4629383. [PubMed: 30050932]

(17). Myneni V; Mezey E Regulation of bone remodeling by vitamin K2. Oral Diseases 2017, 23 (8), 1021–1028. [PubMed: 27976475]

(18). Dasari S; Samy ALPA; Kajdacsy-Balla A; Bosland MC; Munirathinam G Vitamin K2, a menaquinone present in dairy products targets castration-resistant prostate cancer cell-line by activating apoptosis signaling. Food Chem. Toxicol 2018, 115, 218–227. [PubMed: 29432837]

(19). Buchanan GS; Melvin T; Merritt B; Bishop C; Shuler FD Vitamin K2 (menaquinone) Supplementation and its Benefits in Cardiovascular Disease, Osteoporosis, and Cancer. Marshall Journal of Medicine 2016, 2 (3), 53.

(20). Roy M; Bandyopadhyay A; Bose S Induction plasma sprayed Sr and Mg doped nano hydroxyapatite coatings on Ti for bone implant. J. Biomed. Mater. Res., Part B 2011, 99 (2), 258–265.

(21). Bandyopadhyay A; Shivaram A; Tarafder S; Sahasrabudhe H; Banerjee D; Bose S In vivo response of laser processed porous titanium implants for load-bearing implants. Ann. Biomed. Eng 2017, 45 (1), 249–260. [PubMed: 27307009]

(22). Maló P; de Araújo Nobre M; Borges J; Almeida R Retrievable metal ceramic implant-supported fixed prostheses with milled titanium frameworks and all-ceramic crowns: retrospective clinical study with up to 10 years of follow-up. J. Prosthodontics 2012, 21 (4), 256–264.

(23). Brunette DM, Pentti T, Marcus T, Peter T, Eds. Titanium in Medicine: Material Science, Surface Science, Engineering, Biological Responses and Medical Applications; Springer Science & Business Media, 2012.

(24). Tran P; Webster TJ Enhanced osteoblast adhesion on nanostructured selenium compacts for anti-cancer orthopedic applications. Int. J. Nanomed 2008, 3 (3), 391.

(25). Bose S; Tarafder S Calcium phosphate ceramic systems in growth factor and drug delivery for bone tissue engineering: a review. Acta Biomater. 2012, 8 (4), 1401–1421. [PubMed: 22127225]

(26). Boanini E; Torricelli P; Sima F; Axente E; Fini M; Mihailescu IN; Bigi A Strontium and zoledronate hydroxyapatites graded composite coatings for bone prostheses. J. Colloid Interface Sci 2015, 448, 1–7. [PubMed: 25706198]

(27). Monte F; Awad KR; Ahuja N; Kim H; Aswath P; Brotto M; Varanasi VG Amorphous Silicon Oxynitrophosphide Coated Implants Boost Angiogenic Activity of Endothelial Cells. Tissue Eng., Part A 2020, 26, 15–27. [PubMed: 31044666]

(28). Vahabzadeh S; Roy M; Bandyopadhyay A; Bose S Phase stability and biological property evaluation of plasma sprayed hydroxyapatite coatings for orthopedic and dental applications. Acta Biomater. 2015, 17, 47–55. [PubMed: 25638672]

(29). Goodman SB; Yao Z; Keeney M; Yang F The future of biologic coatings for orthopaedic implants. Biomaterials 2013, 34 (13), 3174–3183. [PubMed: 23391496]

(30). Fielding GA; Roy M; Bandyopadhyay A; Bose S Antibacterial and biological characteristics of silver containing and strontium doped plasma sprayed hydroxyapatite coatings. Acta Biomater. 2012, 8 (8), 3144–3152. [PubMed: 22487928]

(31). Ke D; Robertson SF; Dernell WS; Bandyopadhyay A; Bose S Effects of MgO and SiO2 on plasma-sprayed hydroxyapatite coating: an in vivo study in rat distal femoral defects. ACS Appl. Mater. Interfaces 2017, 9 (31), 25731–25737. [PubMed: 28752993]

(32). Ke D; Vu AA; Bandyopadhyay A; Bose S Compositionally graded doped hydroxyapatite coating on titanium using laser and plasma spray deposition for bone implants. Acta Biomater. 2019, 84, 414–423. [PubMed: 30500448]

(33). Vu AA; Robertson SF; Ke D; Bandyopadhyay A; Bose S Mechanical and biological properties of ZnO, SiO2, and Ag2O doped plasma sprayed hydroxyapatite coating for orthopaedic and dental applications. Acta Biomater. 2019, 92, 325–335. [PubMed: 31082568]

(34). Korsmeyer RW; Gurny R; Doelker E; Buri P; Peppas NA Mechanisms of solute release from porous hydrophilic polymers. Int. J. Pharm 1983, 15 (1), 25–35.

(35). Marques C; Ferreira JMF; Andronescu E; Ficai D; Sonmez M; Ficai A Multifunctional materials for bone cancer treatment. Int. J. Nanomed 2014, 9, 2713.

(36). Gao N; Xing C; Wang H; Feng L; Zeng X; Mei L; Peng Z pH-Responsive Dual Drug-Loaded Nanocarriers Based on Poly (2-Ethyl-2-Oxazoline) Modified Black Phosphorus Nanosheets for Cancer Chemo/Photothermal Therapy. Front. Pharmacol 2019, 10, 270. [PubMed: 30941045]

(37). Han Y; He Z; Schulz A; Bronich TK; Jordan R; Luxenhofer R; Kabanov AV Synergistic combinations of multiple chemotherapeutic agents in high capacity poly (2-oxazoline) micelles. Mol. Pharmaceutics 2012, 9 (8), 2302–2313.

(38). Khurana K; Guillem-Marti J; Soldera F; Mucklich F; Canal C; Ginebra M-P Injectable calcium phosphate foams for the delivery of Pitavastatin as osteogenic and angiogenic agent. J. Biomed. Mater. Res., Part B 2019, DOI:10.1002/jbm.b.34430.

(39). Cao J; Chen Z; Chi J; Sun Y; Sun Y Recent progress in synergistic chemotherapy and phototherapy by targeted drug delivery systems for cancer treatment. Artif. Cells, Nanomed., Biotechnol 2018, 46 (sup1), 817–830.

(40). Habu D; Shiomi S; Tamori A; Takeda T; Tanaka T; Kubo S; Nishiguchi S Role of vitamin K2 in the development of hepatocellular carcinoma in women with viral cirrhosis of the liver. Journal of the American Medical Association 2004, 292 (3), 358–361. [PubMed: 15265851]

(41). Kiely M; Hodgins SJ; Merrigan BA; Tormey S; Kiely PA; O'Connor EM Real-time cell analysis of the inhibitory effect of vitamin K2 on adhesion and proliferation of breast cancer cells. Nutr. Res 2015, 35 (8), 736–743. [PubMed: 26082424]

(42). Kim JH; Gupta SC; Park B; Yadav VR; Aggarwal BB Turmeric (Curcuma longa) inhibits inflammatory nuclear factor (NF)-κB and NF-κB-regulated gene products and induces death receptors leading to suppressed proliferation, induced chemosensitization, and suppressed osteoclastogenesis. Mol. Nutr. Food Res 2012, 56 (3), 454–465. [PubMed: 22147524]

(43). Park M; Hong J Roles of NF-κB in cancer and inflammatory diseases and their therapeutic approaches. Cells 2016, 5 (2), 15.

(44). Gupta SC; Patchva S; Aggarwal BB Therapeutic roles of curcumin: lessons learned from clinical trials. AAPS J. 2013, 15 (1), 195–218. [PubMed: 23143785]

(45). Yang H; Gu Q; Huang C; Cai Y; Shi Q Curcumin increases rat mesenchymal stem cell osteoblast differentiation but inhibits adipocyte differentiation. Pharmacogn. Mag 2012, 8 (31), 202. [PubMed: 23060694]

(46). Chang R; Sun L; Webster T Selective inhibition of MG-63 osteosarcoma cell proliferation induced by curcumin-loaded self-assembled arginine-rich-RGD nanospheres. Int. J. Nanomed 2015, 10, 3351.

(47). Wen L; Chen J; Duan L; Li S Vitamin K-dependent proteins involved in bone and cardiovascular health. Mol. Med. Rep 2018, 18 (1), 3–15. [PubMed: 29749440]

(48). Giri TK; Newton D; Chaudhary O; Deych E; Napoli N; Villareal R; Diemer K; Milligan PE; Gage BF Maximal dose-response of vitamin-K2 (menaquinone-4) on undercarboxylated osteocalcin in women with osteoporosis. Int. J. Vitam. Nutr. Res 2020, 90, 42–48. [PubMed: 30816822]

(49). Yamaguchi M; Weitzmann MN Vitamin K2 stimulates osteoblastogenesis and suppresses osteoclastogenesis by suppressing NF-μB activation. Int. J. Mol. Med 2010, 27 (1), 3–14. [PubMed: 21072493]

(50). Bose S; Sarkar N; Banerjee D Effects of PCL, PEG and PLGA polymers on curcumin release from calcium phosphate matrix for in vitro and in vivo bone regeneration. Materials Today Chemistry 2018, 8, 110–120. [PubMed: 30480167]

(51). He R; Hu X; Tan HC; Feng J; Steffi C; Wang K; Wang W Surface modification of titanium with curcumin: a promising strategy to combat fibrous encapsulation. J. Mater. Chem. B 2015, B3 (10), 2137–2146.

(52). Cirano FR; Pimentel SP; Casati MZ; Corrêa MG; Pino DS; Messora MR; Silva PHF; Ribeiro FV Effect of curcumin on bone tissue in the diabetic rat: repair of peri-implant and critical-sized defects. International journal of oral and maxillofacial surgery 2018, 47 (11), 1495–1503. [PubMed: 29857981]

(53). Li B; Hu Y; Zhao Y; Cheng M; Qin H; Cheng T; Wang Q; Peng X; Zhang X Curcumin attenuates titanium particle-induced inflammation by regulating macrophage polarization in vitro and in vivo. Front. Immunol 2017, 8, 55. [PubMed: 28197150]

(54). Atkins GJ; Welldon KJ; Wijenayaka AR; Bonewald LF; Findlay DM Vitamin K promotes mineralization, osteoblast-to-osteocyte transition, and an anticatabolic phenotype by γ-carboxylation-dependent and-independent mechanisms. American Journal of Physiology-Cell Physiology 2009, 297 (6), C1358–C1367. [PubMed: 19675304]

(55). Li H; Zhou Q; Bai B-L; Weng S-J; Wu Z-Y; Xie Z-J; Feng Z-H; Cheng L; Boodhun V; Yang L Effects of combined human parathyroid hormone (1–34) and menaquinone-4 treatment on the interface of hydroxyapatite-coated titanium implants in the femur of osteoporotic rats. J. Bone Miner. Metab 2018, 36 (6), 691–699. [PubMed: 29280077]

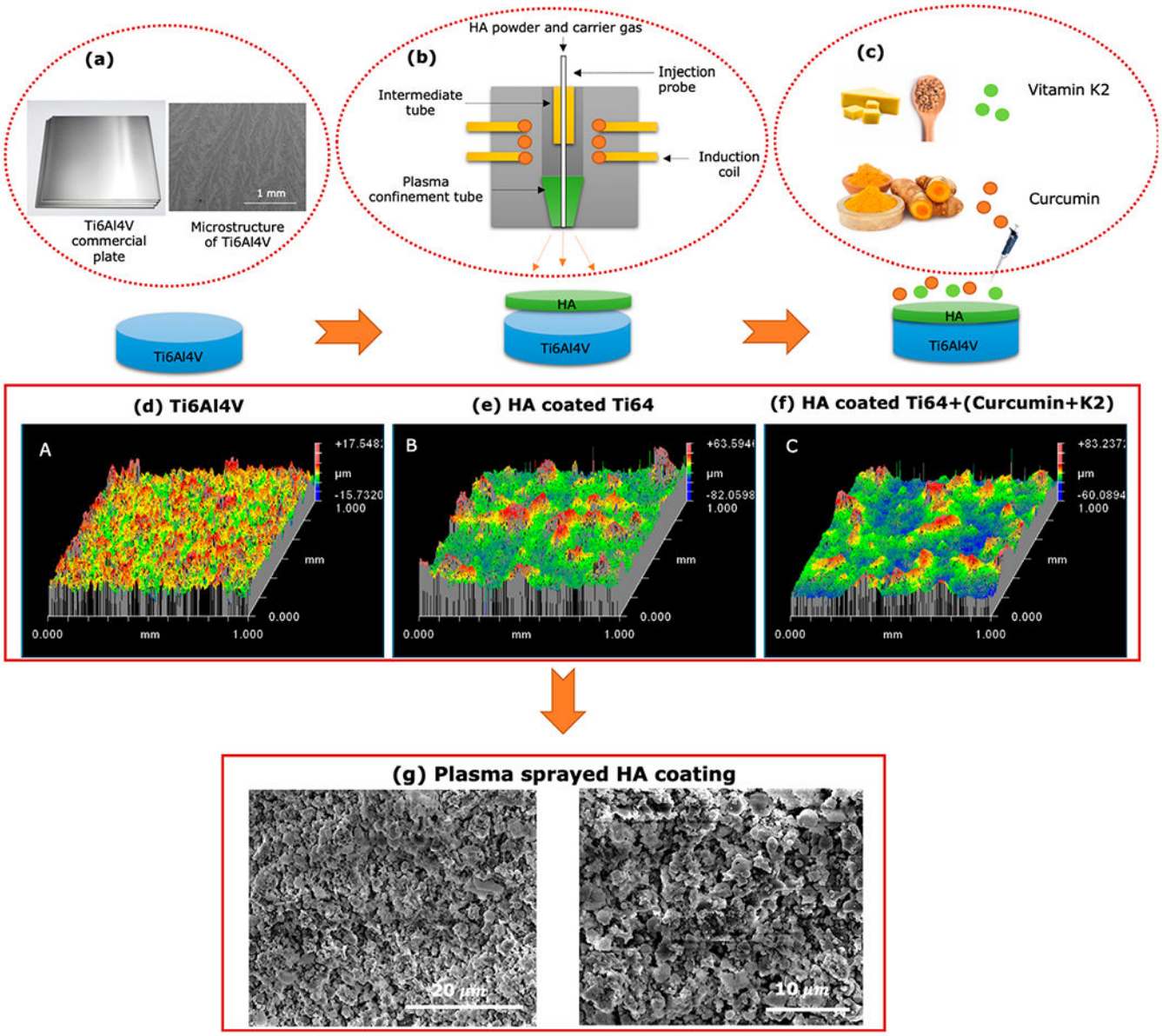

Figure 1.

Step by step fabrication procedure for drug-loaded HA-coated implants. (a) Microstructure of the Ti alloy substrate by FESEM. (b) Simple schematic illustration of plasma spraying process for depositing HA powder and (c) dual-drug loading on HA coated Ti6Al4V implant. Profilometry data demonstrating the surface topography of (d) Ti6Al4V, (e) HA-coated Ti6Al4V, and (f) drug-loaded HA-coated Ti6Al4V. (g) FESEM images showing surface morphology of as-prepared plasma sprayed HA coating on Ti6Al4V implant.

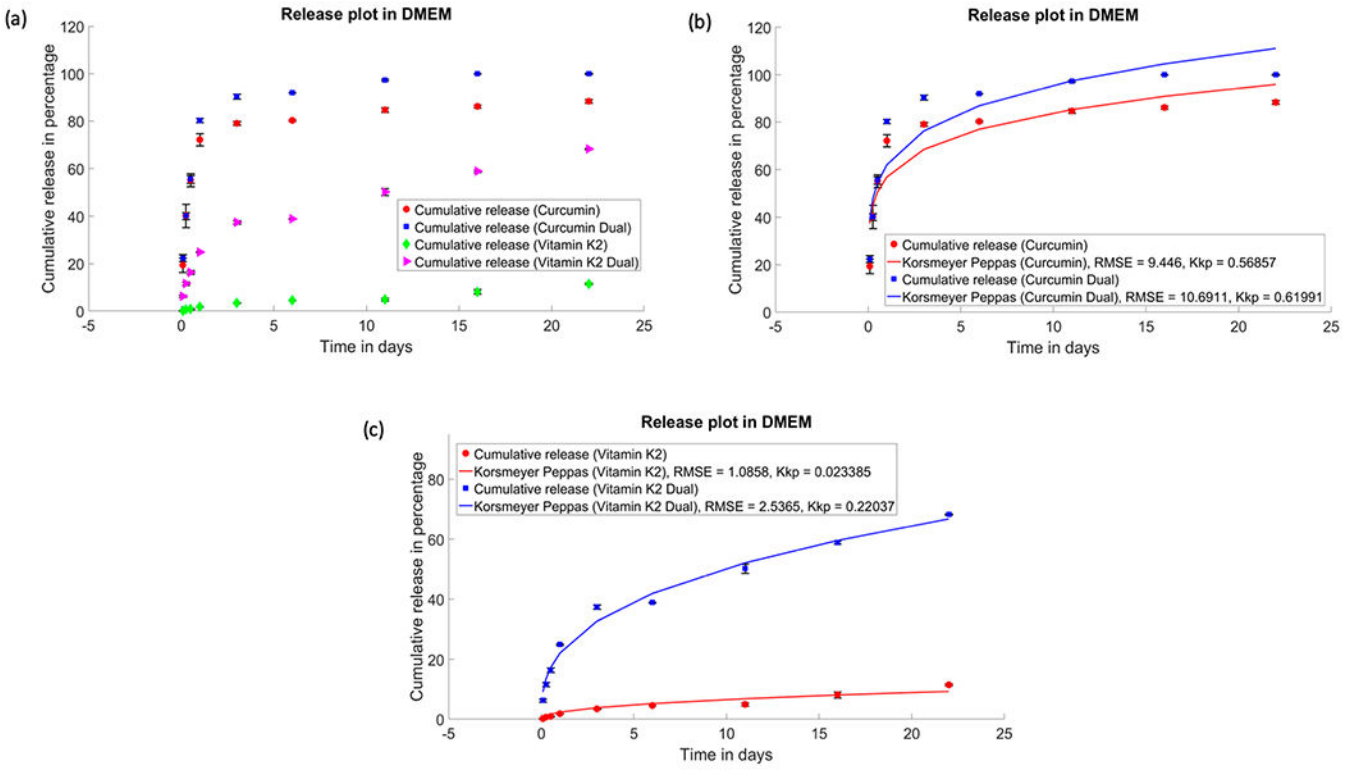

Figure 2.

Drug release profiles of curcumin, vitamin K2, and curcumin + vitamin K2 from plasma-sprayed HA-coated Ti implant for 22 days: (a) In vitro release of curcumin and vitamin K2 individually and in the presence of each other under pH 7.4 (DMEM). Cumulative release kinetics of curcumin (b) and vitamin K2 (c), respectively, fitted with Korsmeyer–Peppas model ($p \leq 0.05$).

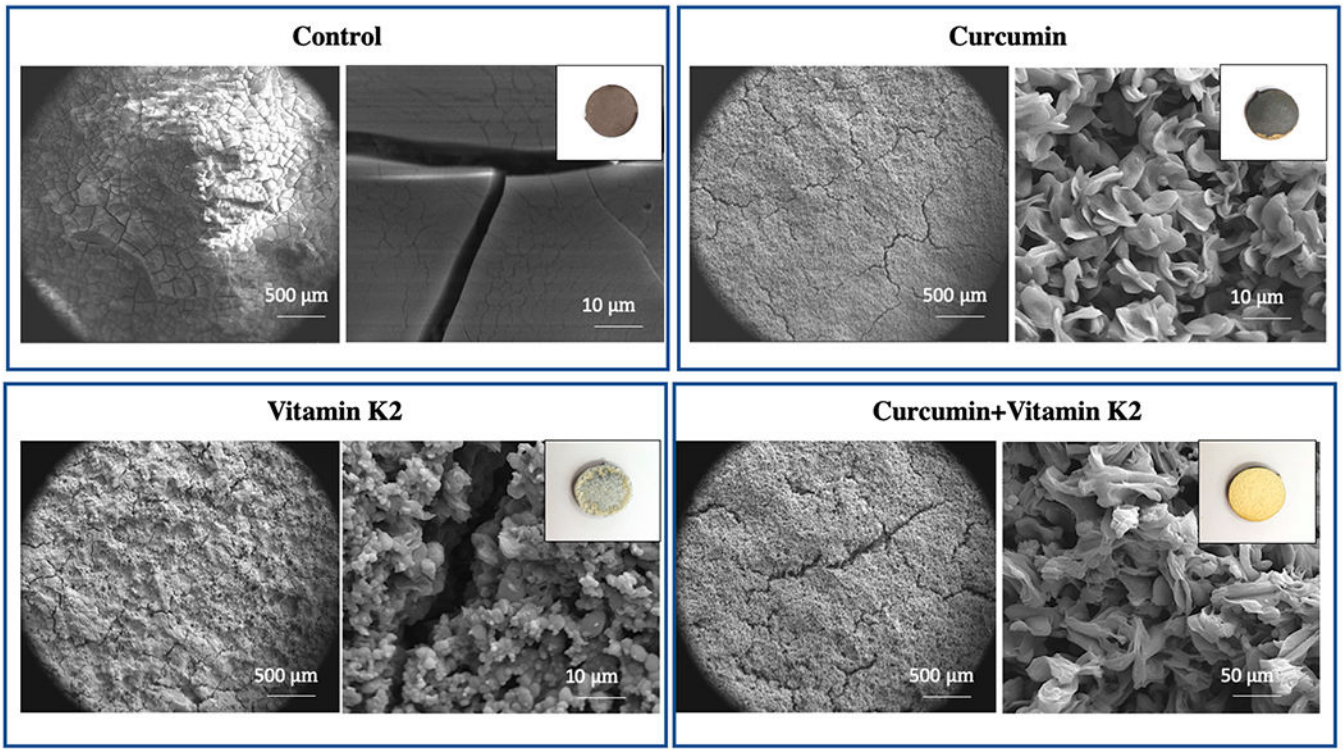

Figure 3.

Morphology of sample surface control, curcumin, vitamin K2, curcumin + vitamin K2 after drug release for 22 days under pH 7.4 (DMEM). (Images of samples after 22 days of drug release show surface and coating degradation.) Data were expressed as mean ± SD [$n = 3$].

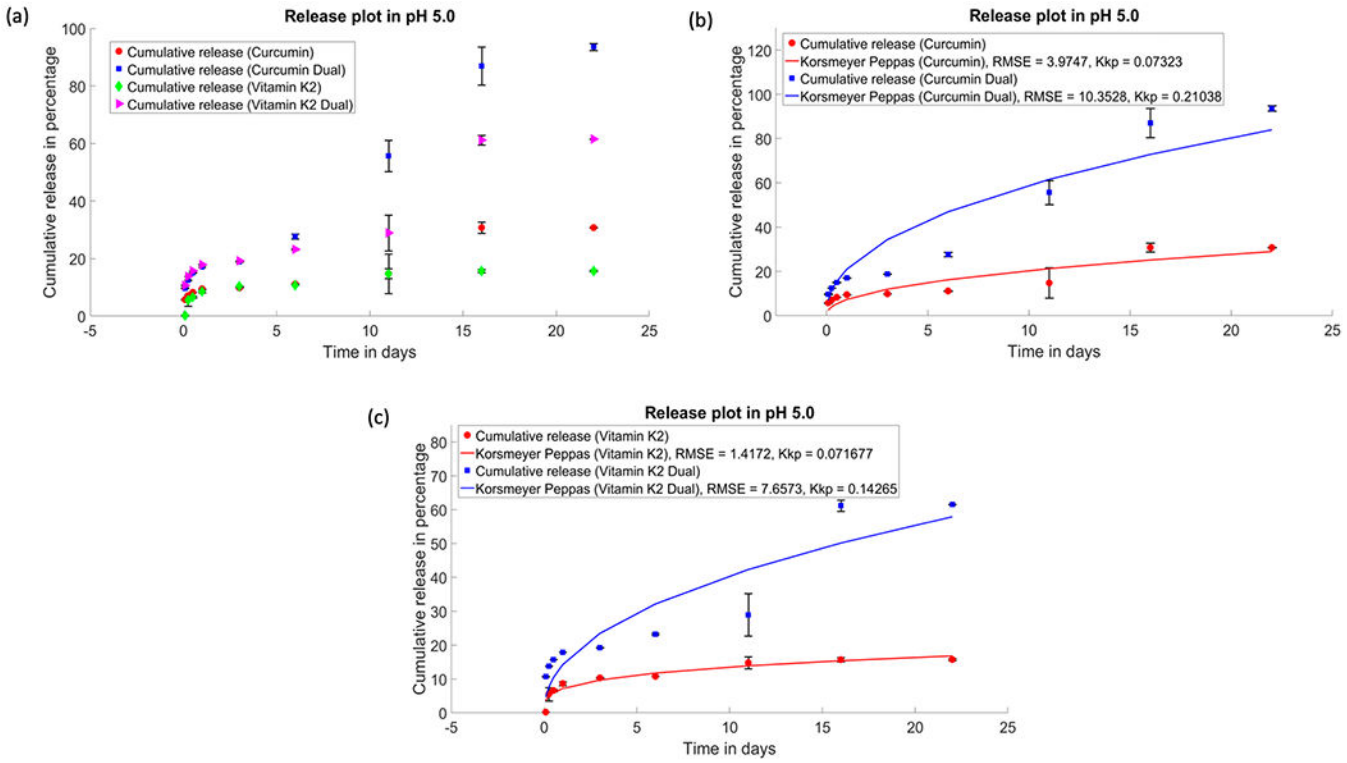

Figure 4.

Drug release profiles of curcumin, vitamin K2, and curcumin + vitamin K2 from plasma-sprayed HA-coated Ti implant for 22 days: (a) in vitro release of curcumin and vitamin K2 individually and in the presence of each other under pH 5.0 and cumulative release kinetics of curcumin (b) and vitamin K2 (c), respectively, fitted with the Korsmeyer–Peppas model ($p \leq 0.05$).

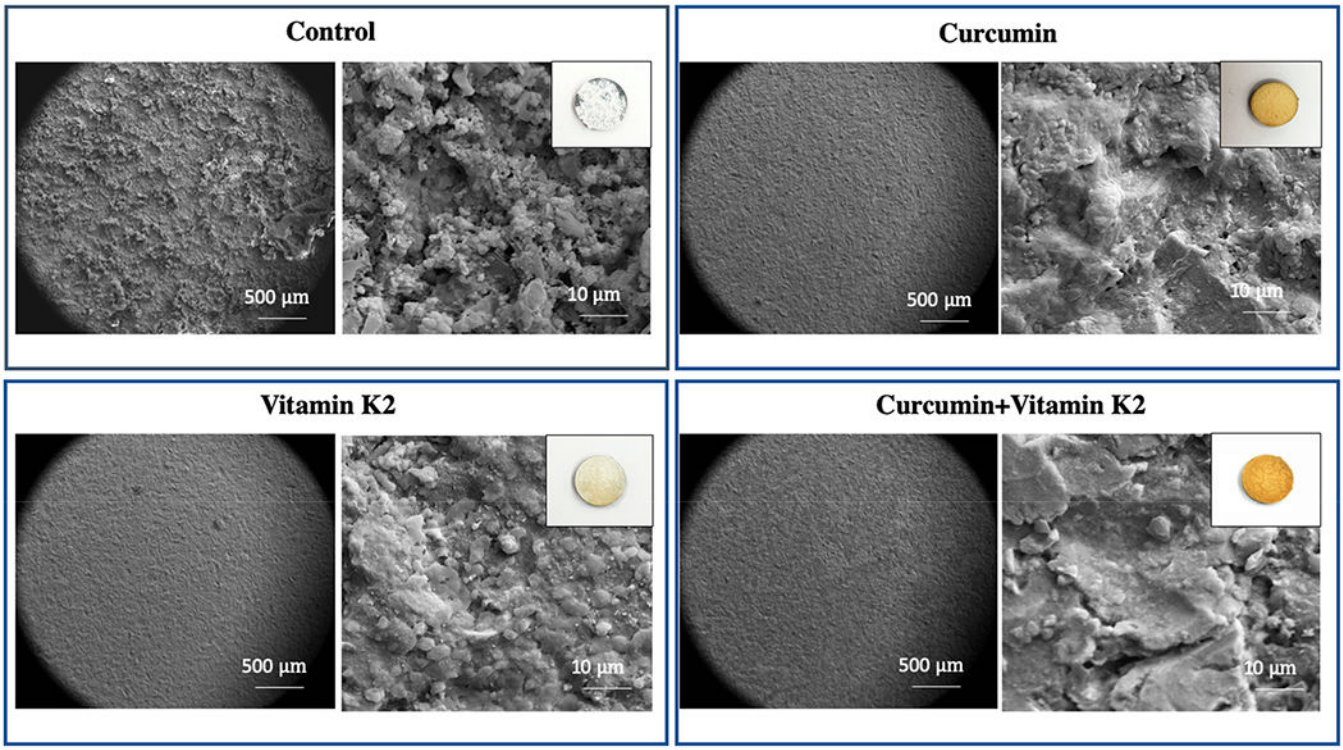

Figure 5.

Morphology of sample surface control, curcumin, vitamin K2, and curcumin + vitamin K2 after drug release for 22 days under pH 5.0 (acetate buffer). (Images of samples after 22 days of drug release show surface and coating degradation.) Data were expressed as mean ± SD [$n = 3$].

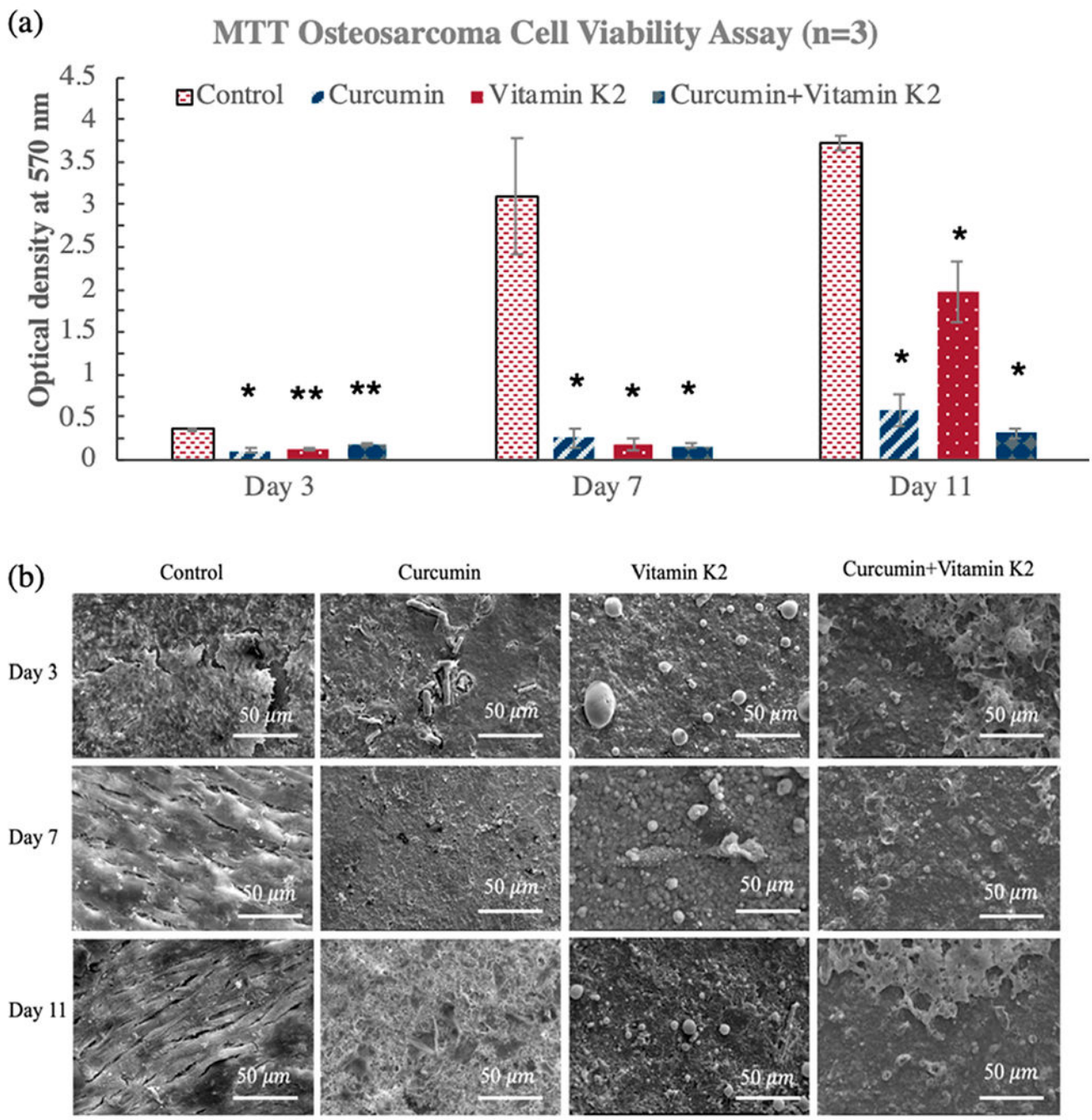

Figure 6.

In vitro cytotoxicity assay against osteosarcoma (MG-63) cells using curcumin-, vitamin K2-, and curcumin + vitamin K2-loaded HA-coated Ti implants at days 3, 7, and 11. (a) MTT assay showing the effects of curcumin, vitamin K2, and curcumin + vitamin K2 on osteosarcoma cell viability (* denotes $p \leq 0.001$, ** denotes $p \leq 0.05$). (b) Morphological characterization by FESEM showing the osteosarcoma cell attachment and proliferation on curcumin-, vitamin K2-, and curcumin + vitamin K2-loaded HA-coated Ti implant surface.

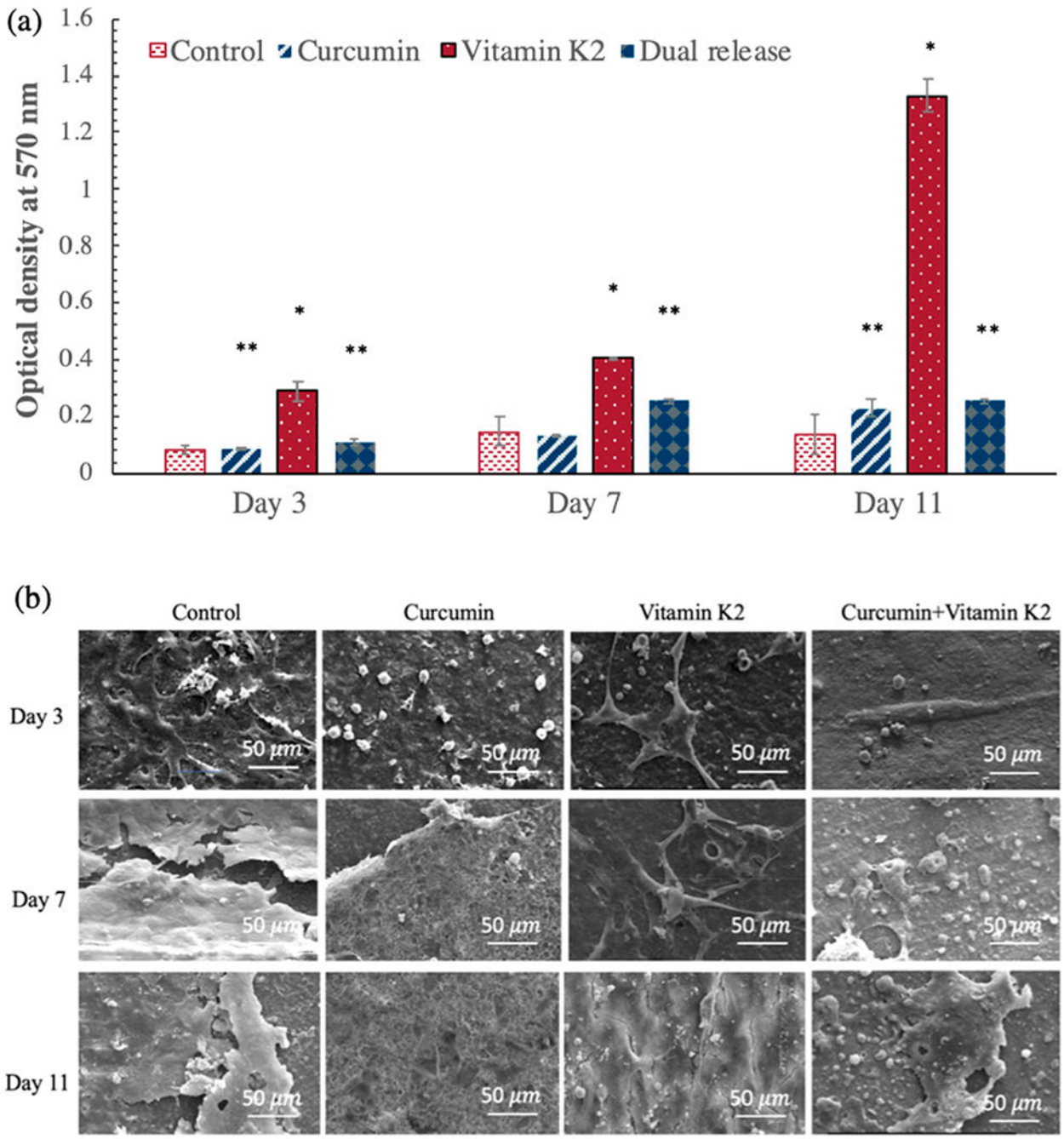

Figure 7.

In vitro cell viability assay for osteoblast (hFOB) cells with curcumin-, vitamin K2-, and curcumin + vitamin K2-loaded HA-coated Ti implants at days 3, 7, and 11. (a) MTT assay showing the effects of curcumin, vitamin K2, and curcumin + vitamin K2 on osteoblast cell viability (* denotes $p \leq 0.001$, ** denotes $p \leq 0.05$). (b) Morphological characterization by FESEM showing the osteoblast cell attachment and proliferation on curcumin-, vitamin K2-, and curcumin + vitamin K2-loaded HA-coated Ti implant surface.

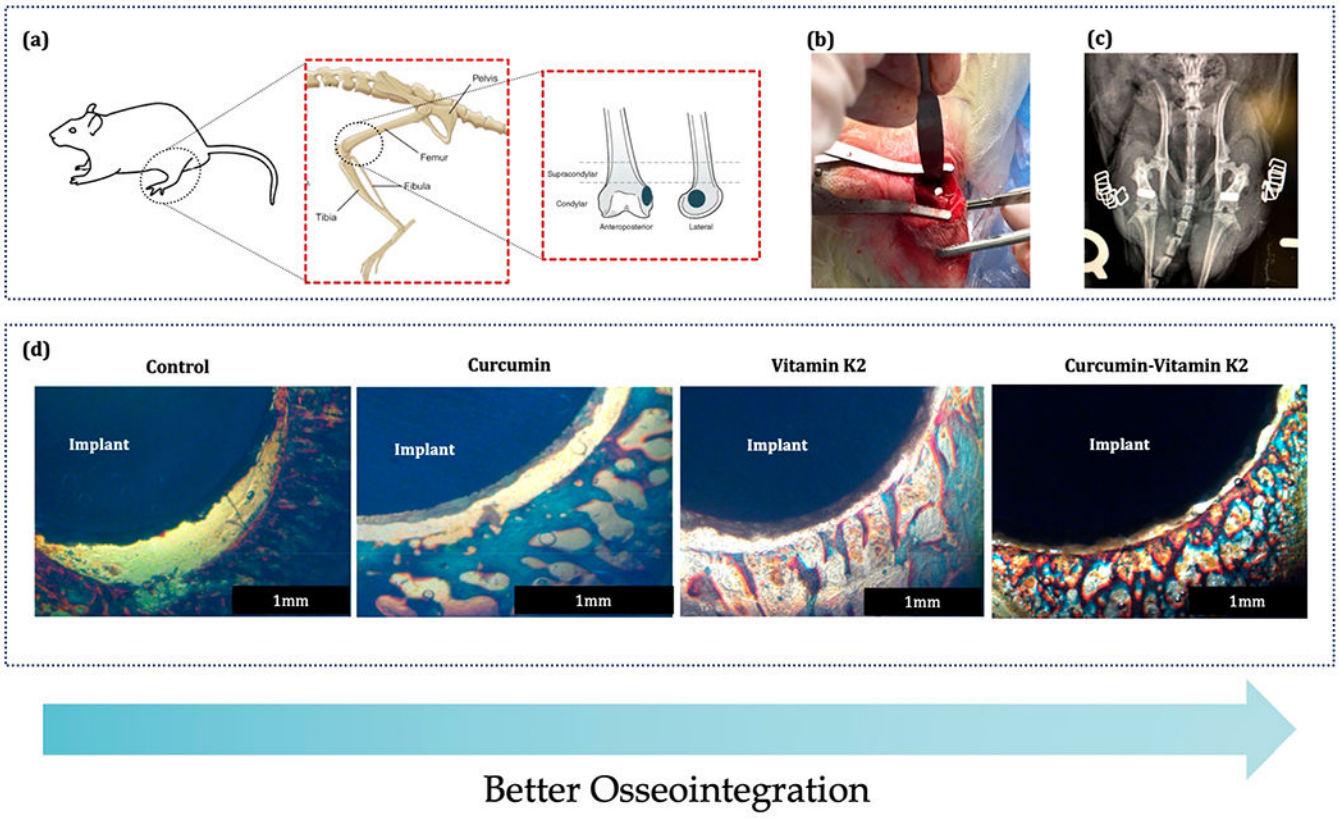

Figure 8.

In vivo surgical procedure and bone bonded zone shown by Masson Goldner staining: (a) 3/5 mm defect location at the lower epicondyle of the rat distal femur model, (b) implantation procedure, (c) postsurgical radiograph showing the placement of implant, and (d) Masson Goldner staining showing the implant and surrounding bone after sacrificing the rats at 5 days (n = 4).

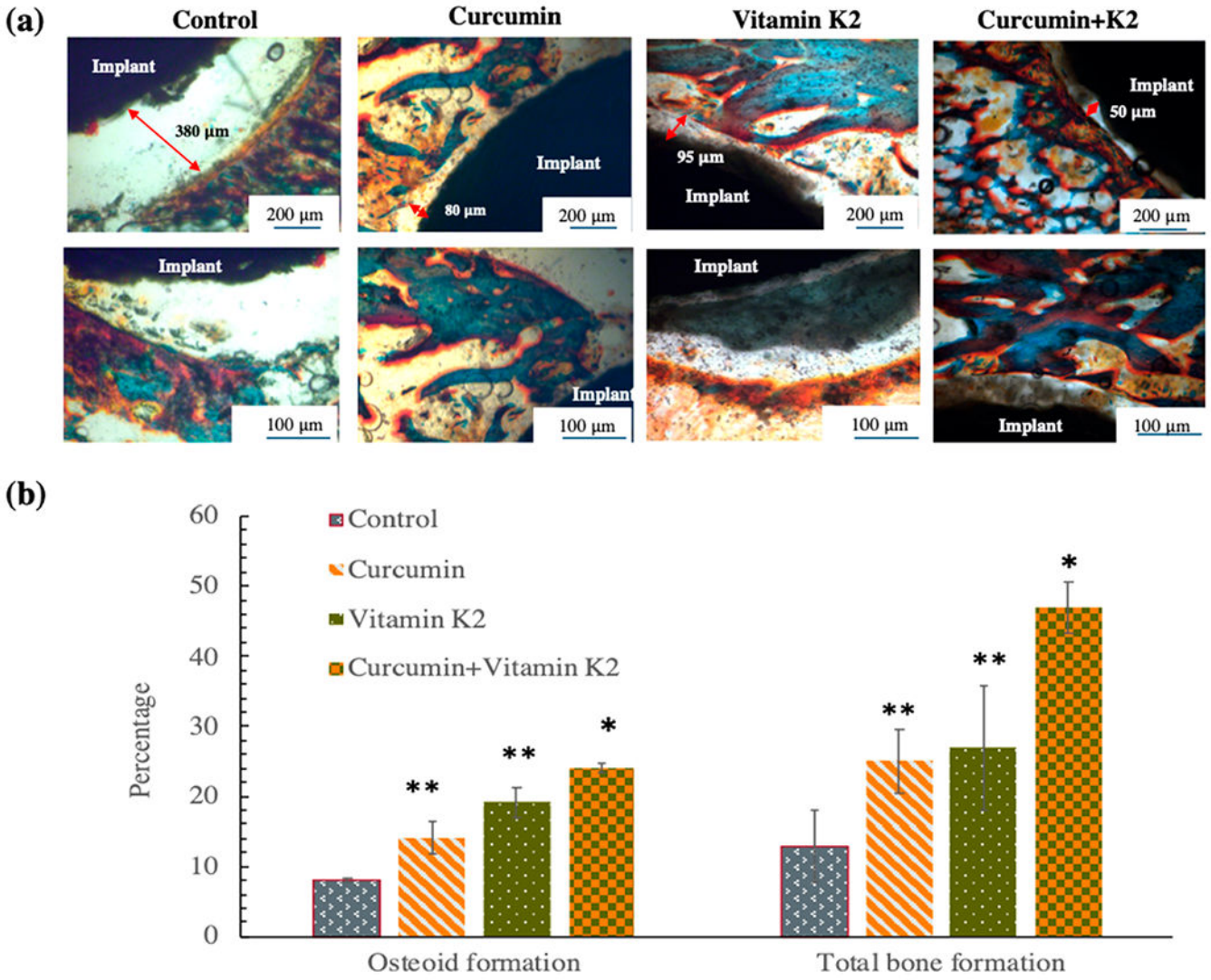

Figure 9.

(a) In vivo Masson Goldner staining by curcumin-, vitamin K2-, and curcumin + vitamin K2-loaded HA-coated Ti implant showing the gap between the implant and the surrounding bone tissue after 5 days of implantation at rat distal femur model. The new bone formation or osteoid tissue is stained with red/orange; mineralized bone tissue is stained with green/blue, and the implant can be seen in black. (b) Histomorphometric analysis by ImageJ software showing percentage osteoid or new bone tissue formation and percentage total bone formation within 250 μm radius of implant after 5 days. Drug-loaded implant exhibited statistically significant difference in osteoid formation and total bone formation after 5 days indicating better osseointegration ability compared to the control (*$p < 0.001$, **$p < 0.05$).

Table 1.

Surface Topography Measurements of Ti6Al4V, HA-Coated Ti Implant, and Curcumin + Vitamin K2-Loaded HA-Coated Ti Implant ($n = 3$)

	mean roughness R_a (μm)	maximum height R_z (μm)	RMS roughness (μm)
Ti6Al4V	2.353	33.29	2.998
HA-coated Ti implant	10.43	145.6	13.83
curcumin + vitamin K2-loaded HA-coated Ti implant	8.61	143.2	10.98

Table 2.

Release Kinetics Parameters Fitted from Korsmeyer–Peppas Model

composition	*n*	R^2
curcumin-loaded Ti implant (DMEM, pH 7.4)	0.1692	0.9091
vitamin K2-loaded Ti implant (DMEM, pH 7.4)	0.4458	0.9685
curcumin-loaded Ti implant (pH 5.0)	0.4452	0.9087
vitamin K2-loaded Ti implant (pH 5.0)	0.2762	0.9588
curcumin release from dual drug-loaded implant (DMEM, pH 7.4)	0.1886	0.9196
vitamin K2 release from dual drug-loaded implant (DMEM, pH 7.4)	0.3585	0.9924
curcumin release from dual drug-loaded implant (pH 5.0)	0.4477	0.9490
vitamin K2 release from dual drug-loaded implant (pH 5.0)	0.4532	0.9159

Table 3.

Cytotoxicity Potential against Osteosarcoma Cells by Curcumin-, Vitamin K2-, and Curcumin + Vitamin K2-Loaded HA-Coated Ti Implant at Days 3, 7, and 11[a].

	curcumin	vitamin K2	curcumin + vitamin K2
day 3	29.19	36.78	50.05
day 7	8.27	6.07	5.35
day 11	15.79	53.10	8.37

[a]<70% implies the drug has cytotoxic potential.